XXVIIth International Conference on Ultrarelativistic Nucleus-Nucleus Collisions
(Quark Matter 2018)

Electroweak probes of small and large systems with the ATLAS detector

Zvi Citron for the ATLAS Collaboration

Ben Gurion University of the Negev

Abstract

Measurements of isolated prompt photon and massive electroweak (*W* and *Z*) boson production in different collision systems are of great interest to understand the partonic structure of heavy nuclei, and serve as a constraint on the initial state in larger collision systems. These channels are sensitive to a variety of effects such as the modification of the parton densities in nuclei in certain kinematic regions, and the energy loss of partons as they undergo multiple interactions in the nucleus before the hard parton-parton scattering. High-statistics samples of lead–lead and proton–lead collision data at $\sqrt{s_{NN}}$=5.02 TeV and 8.16 TeV, respectively, taken by the ATLAS experiment at the LHC, as well as proton–proton comparison data at analogous collision energies, allow for a detailed study of these phenomena in data and comprehensive comparisons to the predictions of a variety of theoretical approaches. This paper presents the latest ATLAS results in these topics, including updated results on inclusive prompt photon production in proton–lead collisions over a broad kinematic range and high-precision *W* boson results in lead–lead collisions.

Keywords: Lead–lead collisions, Proton–lead collisions, Proton–proton collisions, Photons, *W* boson, *Z* boson

1. Introduction

Electroweak bosons are a valuable tool to study the hot and dense medium created in heavy-ion collisions. Since they and their leptonic decay products are insensitive to the strong force and do not interact with the QCD medium, the rate of their production in different centrality classes allows a test of binary collision scaling within heavy ion (HI) collisions. In addition, they are well suited to serve as probes of nuclear modification of the parton distribution function within the relativistic ion.

The ATLAS experiment [1] measured the EW boson production in pp, p+Pb and Pb+Pb collisions at the LHC. The former offers a high precision test of pQCD as well as a baseline for heavy-ion collisions. Measurements in *pp* collisions offer a high precision test of pQCD as well as a baseline for p+Pb, and Pb+Pb collisions. Proton–lead collisions are an optimal system in which to study modifications of the initial nuclear state relative to free nucleons. Electroweak bosons in Pb+Pb collisions, in which a quark gluon plasma is thought to be produced, function as a 'standard candle' by which to gauge effects of the plasma.

2. Z Bosons in Proton–Proton Collisions

The analysis of Z bosons in 25 pb^{-1} of pp collisions with $\sqrt{s}$ = 5.02 TeV is described in detail in [2]. Z boson candidates were reconstructed in the di-muon decay channel. Events are selected using a single muon trigger with transverse momentum above 14 GeV. Candidate events are required to have two high-quality opposite charge muons each with p$_T$ >20 GeV and $|\eta|$ <2.4. There are 7293 events selected with di-muon invariant mass between 66 and 116 GeV. Background processes, chiefly $Z \to \tau\tau$ and $t\bar{t}$, total approximately 0.3% of the events and their contribution is subtracted. The data are fully corrected for trigger and reconstruction efficiency as well as detector acceptance. The cross section for the mass window 66< m_Z <116 GeV and rapidity $|y^Z|$ <2.5 is measured to be 590 ± 9 (stat.) ± 12 (stat.) ± 32 (lumi.) pb. The measurement serves as a robust baseline to the measurements made in heavy–ion collisions.

3. Photons in Proton–Lead Collisions

The analysis of isolated photons in 162 nb^{-1} of p+Pb collisions with $\sqrt{s_{NN}}$ = 8.16 TeV is described in detail in [3]. Photons are identified based on shower shapes in the calorimeter that are consistent with a single photon. A selection of isolated photons reduces background from fragmentation and decay photons and is achieved by excluding events in which there is energy above a certain threshold within a cone of η and ϕ around the measured photon.

The transverse energy, E_T, differential cross-section is constructed as:

$$d\sigma/dE_T = \frac{1}{L_{int}} \frac{1}{\Delta E_T} \frac{N_{sig} P_{sig}}{\epsilon^{sel} \epsilon^{trig}} C, \tag{1}$$

where L_{int} is the integrated luminosity, N_{sig} is the yield of photon candidates passing identification and isolation requirements, P_{sig} is the purity of signal photons in this selection, ϵ^{sel} is the combined reconstruction, identification and isolation efficiency for signal photons, ϵ^{trig} is the trigger efficiency, and C is a correction for the bin migration in E_T caused by detector inefficiencies and the finite resolution of the photon energy measurement. The purity, P_{sig}, is estimated using the "double sideband" method, in which "off-signal" regions defined as permutations of passing and failing of the isolation and identification selections are used to estimate the background which passes into events selected as isolated signals.

To search for effects of nuclear modification, the E_T differential nuclear modification factor R$_{pPb}$ is defined as:

$$R_{pPb}(E_T) = \frac{1}{A_{Pb}} \frac{d\sigma_{pPb}/dE_T}{d\sigma_{pp}/dE_T}, \tag{2}$$

with the mass number of the lead ion, A$_{Pb}$=208. In order to obtain an appropriate pp spectrum for construction of the R$_{pPb}$, a previous ATLAS measurement at $\sqrt{s}$ = 8 TeV [4] is extrapolated to match the center of mass energy and rapidity boost with respect to the detector of the p+Pb system using JETPHOX [5]. In Figure 1 the measured R$_{pPb}$ is shown and compared to the same quantity calculated using JETPHOX based on the CT14 free proton PDF set [6] with and without the including nuclear modification effects parameterized in the EPPS16 nuclear PDF set [7]. Although there is good reason to expect that electroweak bosons are sensitive to nuclear modification in p+Pb collisions at the LHC [8], these data are not yet able to distinguish between the free proton and nuclear effect modified PDF sets.

4. W and Z Bosons in Lead–Lead Collisions

The analysis of W bosons in Pb+Pb collisions with $\sqrt{s_{NN}}$ = 5.02 TeV is described in detail in [9]. W bosons are measured via the $W^+ \to \mu^+\nu$ and $W^- \to \mu^-\bar{\nu}$ channels; the muon is measured directly and the neutrino is reconstructed by missing transverse momentum in the event. This missing momentum, p$_T^{miss}$, is calculated as the negative vector sum of reconstructed charged particle tracks excepting the muon itself. Candidate events are defined as those with muon p$_T$ >25 GeV, 0.1< $|\eta|$ <2.5 (0< $|\eta|$ <0.1 is excluded due to quickly changing detector performance in this region), p$_T^{miss}$ >25 GeV, and m_T >40 GeV, where
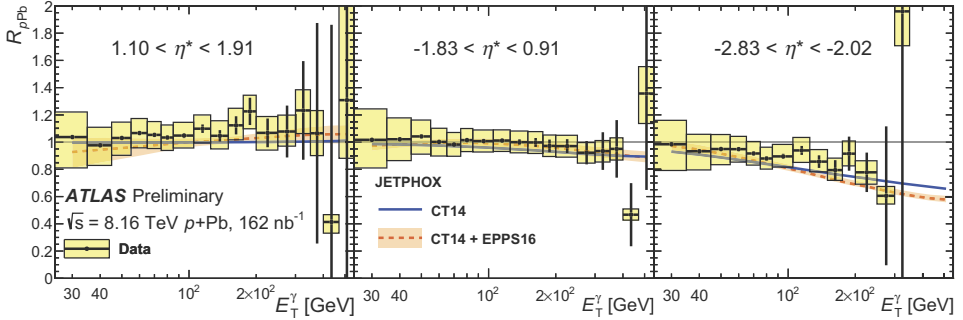
Fig. 1. Nuclear modification factor R_{pPb} for isolated, prompt photons as a function of E_T, shown for different pseudo-rapidity selections in each panel. The data are compared to the expectations based on JETPHOX using the CT14 PDF with and without the EPPS16 nuclear PDF set. The yellow bands and vertical bars correspond to total systematic and statistical uncertainties on the data, respectively. [3]

$m_T = \sqrt{2p_T p_T^{\text{miss}}(1 - cos\Delta\phi)}$ with $\Delta\phi$ the difference in angle between the muon and missing momentum vector. Following these selections there are 25245 positive muons and 23123 negative muon candidate events. Backgrounds contamination of the candidate events is predominantly from QCD multi-jet events, $Z \rightarrow \mu^+\mu^-$, and $W \rightarrow \tau\nu$ processes. These range from 6% to 12% for the multi-jet background and approximately 3% for the Z boson background, estimated using data-driven and simulation based methods and subtracted. The remaining signal is corrected for efficiency and acceptance of the detector into the fiducial volume of the event selection criteria listed above (with $p_T^{\text{miss}} \rightarrow p_T^{\nu}$). The corrected signal is scaled by the nuclear thickness function T_{AA} and the number of sampled minimum bias Pb+Pb collisions in each centrality bin and shown as a function of centrality in the left panel of Figure 2. Alongside the data are shown the expected yields based on a POWHEG [10] calculation using the CT10 [11] free PDF set.
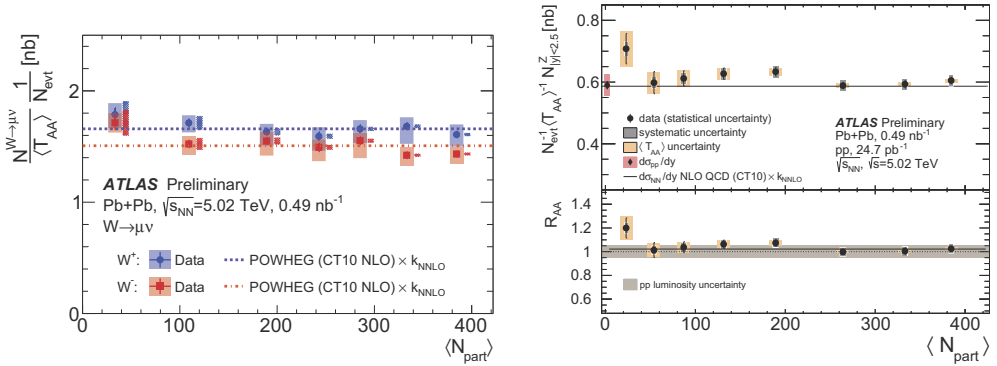

Fig. 2. Left: W^+ (circles) and W^- (squares) boson yield per event divided by T_{AA} as a function of $\langle N_{part} \rangle$, along with model predictions. [9] Right: Z boson yield per event divided by T_{AA} (circles) as a function of $\langle N_{part} \rangle$ and the cross section measured in pp (diamond) plotted at $\langle N_{part} \rangle$ =2, as well as the R_{AA} as a function of $\langle N_{part} \rangle$.[12]

The analysis of Z bosons in Pb+Pb collisions with $\sqrt{s_{NN}} = 5.02$ TeV is described in detail in [12]. Similar to the analysis of pp collisions described above in section 2, Z boson candidates were reconstructed in the di-muon decay channel. Events were selected based on a single muon trigger as for W bosons. Candidate events are required to have two high-quality opposite charge muons each with p_T >20 GeV and $|\eta|$ <2.5 ($|\eta|$ <2.4 for the triggering muon). There are 5326 events selected with di-muon invariant mass between

66 and 116 GeV. Estimated background, amounting to less than 1%, is subtracted and the remaining signal is corrected for detector efficiency and acceptance as above. The measured Z boson yield is scaled by T_{AA} and the number of sampled minimum bias Pb+Pb collisions in each centrality bin and then divided by the cross-section measured in pp collisions, to form the centrality dependent nuclear modification factor:

$$R_{AA}(\langle N_{part}\rangle) = \frac{N_{\text{PbPb}}(\langle N_{part}\rangle)}{\sigma_{pp} \times T_{AA}(\langle N_{part}\rangle)N_{evt}(\langle N_{part}\rangle)}. \qquad (3)$$

The right panel of Figure 2 shows the centrality dependence of the Z boson yield and $R_{AA}(\langle N_{part}\rangle)$.

The electroweak boson yields in Pb+Pb collisions are consistent with T_{AA} scaling within the uncertainty of the measurements. The precision study of electroweak boson production as a function of centrality may enable interesting new approaches to existing questions in the field. For example, a recent calculation of a centrality bias in peripheral collisions [13] identifies electroweak bosons as a way to experimentally verify the calculated bias, and so a precision measurement in the most peripheral bins could confirm or limit the applicability of the model. Further, both W and Z boson measurements presented here individually have uncertainty comparable to the model based T_{AA} calculations. This suggests the possibility to combine them and measure the production of other observables relative to electroweak bosons via the double ratio R_{AA}^{X}/R_{AA}^{EW}. To the extent that binary scaling is broken in electroweak boson production due to initial state effects this double ratio would incorporate that in its normalization and these effects are expected to depend on x and Q^2 which are different for different bosons and probes. Nevertheless, given the size of the relevant effects on the integrated yields this quantity may serve as wholly data-driven complement to Glauber model R_{AA} calculations.

5. Summary

The ATLAS experiment has measured Z bosons in pp collisions with $\sqrt{s} = 5.02$ TeV, W and Z bosons in Pb+Pb collisions with $\sqrt{s_{NN}} = 5.02$ TeV, and photons in p+Pb collisions with $\sqrt{s_{NN}} = 8.16$ TeV. These are a valuable input for understanding the initial nuclear state of heavy ions, and a reference for HI collisions.

References

[1] ATLAS Collaboration, The ATLAS Experiment at the CERN Large Hadron Collider, JINST 3 (2008) S08003. doi:10.1088/1748-0221/3/08/S08003.

[2] ATLAS Collaboration, Z Boson Production in pp Collisions at $\sqrt{s}$ = 5.02 TeV with the ATLAS detector at the LHC (ATLAS-CONF-2016-107). doi:https://cds.cern.ch/record/2220375.

[3] ATLAS Collaboration, Prompt photon production in $\sqrt{s_{NN}}$ = 8.16 TeV p+Pb collisions with ATLAS (ATLAS-CONF-2017-072). doi:https://cds.cern.ch/record/2285810.

[4] ATLAS Collaboration, Measurement of the inclusive isolated prompt photon cross section in pp collisions at $\sqrt{s}$ = 8 TeV with the ATLAS detector, JHEP 08 (2016) 005. arXiv:1605.03495, doi:10.1007/JHEP08(2016)005.

[5] P. Aurenche, M. Fontannaz, J.-P. Guillet, E. Pilon, M. Werlen, A New critical study of photon production in hadronic collisions, Phys. Rev. D73 (2006) 094007. arXiv:hep-ph/0602133, doi:10.1103/PhysRevD.73.094007.

[6] S. Dulat, T.-J. Hou, J. Gao, M. Guzzi, J. Huston, P. Nadolsky, J. Pumplin, C. Schmidt, D. Stump, C. P. Yuan, New parton distribution functions from a global analysis of quantum chromodynamics, Phys. Rev. D93 (3) (2016) 033006. arXiv:1506.07443, doi:10.1103/PhysRevD.93.033006.

[7] K. J. Eskola, P. Paakkinen, H. Paukkunen, C. A. Salgado, EPPS16: Nuclear parton distributions with LHC data, Eur. Phys. J. C77 (3) (2017) 163. arXiv:1612.05741, doi:10.1140/epjc/s10052-017-4725-9.

[8] ATLAS Collaboration, Z boson production in p+Pb collisions at $\sqrt{s_{NN}}$ = 5.02 TeV measured with the ATLAS detector, Phys. Rev. C92 (4) (2015) 044915. arXiv:1507.06232, doi:10.1103/PhysRevC.92.044915.

[9] ATLAS Collaboration, Measurement of W boson production in the muon channel in Pb+Pb collisions at $\sqrt{s_{NN}}$ =5.02 TeV (ATLAS-CONF-2017-067). doi:https://cds.cern.ch/record/2285571.

[10] S. Alioli, P. Nason, C. Oleari, E. Re, NLO vector-boson production matched with shower in POWHEG, JHEP 07 (2008) 060. arXiv:0805.4802, doi:10.1088/1126-6708/2008/07/060.

[11] H.-L. Lai, M. Guzzi, J. Huston, Z. Li, P. M. Nadolsky, J. Pumplin, C. P. Yuan, New parton distributions for collider physics, Phys. Rev. D82 (2010) 074024. arXiv:1007.2241, doi:10.1103/PhysRevD.82.074024.

[12] ATLAS Collaboration, Z boson production in Pb+Pb collisions at $\sqrt{s_{NN}}$= 5.02 TeV with the ATLAS detector at the LHC (ATLAS-CONF-2017-010). doi:https://cds.cern.ch/record/2244821.

[13] C. Loizides, A. Morsch, Absence of jet quenching in peripheral nucleus-nucleus collisions, Physics Letters B 773 (2017) 408 – 411. doi:https://doi.org/10.1016/j.physletb.2017.09.002.